Hormone sensitive lipase preferentially redistributes to perilipin-5 lipid droplets in human skeletal muscle during moderate-intensity exercise.

Katie L Whytock, Sam O Shepherd, Anton JM Wagenmakers and Juliette A Strauss

Research Institute for Sport and Exercise Science, Liverpool John Moores University, Liverpool L3 3AF

Corresponding Author:

Juliette A Strauss

Research Institute for Sport and Exercise Science,

Liverpool John Moores University,

Liverpool L3 3AF

T: 01519046215

E: j.a.strauss@ljmu.ac.uk

Running Title: HSL redistributes to PLIN5+ LD during moderate-intensity exercise

Key Words: Muscle, Lipid, Lipase

Katie Whytock is a PhD student at the Research Institute of Sport and Exercise Science at Liverpool John Moores University. Her research mainly focuses on the effects of exercise and nutrition on skeletal muscle lipid metabolism and how this links to skeletal muscle insulin resistance. She has a particular interest in the proteins associated with skeletal muscle lipid droplets and how they influence storage and utilisation of intramuscular triglyceride stores.

This is an Accepted Article that has been peer-reviewed and approved for publication in the The Journal of Physiology, but has yet to undergo copy-editing and proof correction. Please cite this article as an 'Accepted Article'; doi: 10.1113/JP275502.

Key Points

- Hormone-sensitive lipase (HSL) and adipose triglyceride lipase (ATGL) are the key enzymes involved in intramuscular triglyceride (IMTG) lipolysis. In isolated rat skeletal muscle, HSL translocates to IMTG-containing lipid droplets (LD) following electrical stimulation. Whether HSL translocation occurs in human skeletal muscle during moderate-intensity exercise is currently unknown.
- Perilipin-2 (PLIN2) and perilipin-5 (PLIN5) have been implicated in regulating IMTG lipolysis by interacting with HSL and ATGL in cell culture and rat skeletal muscle studies.
- This study investigated the hypothesis that HSL (but not ATGL) redistributes to LD during moderate-intensity exercise in human skeletal muscle, and whether the localisation of these lipases with LDs was affected by the presence of PLIN proteins on the LD.

- HSL preferentially redistributed to PLIN5-associated LD whereas ATGL distribution was not altered with exercise.
- This is the first study to illustrate the pivotal step of HSL redistribution to PLIN5-associated LD following moderate-intensity exercise in human skeletal muscle.

Abstract

Hormone-sensitive lipase (HSL) and adipose triglyceride lipase (ATGL) control skeletal muscle lipolysis. ATGL is present on the surface of lipid droplets (LD) containing intramuscular triglyceride (IMTG) in both the basal state and during exercise. HSL translocates to LD in *ex vivo* electrically stimulated rat skeletal muscle. Perilipin-2 and perilipin-5 associated lipid droplets (PLIN2+ and PLIN5+ LD) are preferentially depleted during exercise in humans indicating these PLINs may control muscle lipolysis. We aimed to test the hypothesis that in human skeletal muscle *in vivo* HSL (but not ATGL) is redistributed to PLIN2+ and PLIN5+ LD during moderate-intensity exercise. Muscle biopsies from 8 lean trained males (age 21±1 years, BMI 22.6±1.2 kg.m^{-2} and $\dot{V}o_{2peak}$ 48.2±5.0 ml.min^{-1}.kg^{-1}) were obtained before and immediately following 60 min of cycling exercise at ~59% $\dot{V}o_{2peak}$. Cryosections were stained using antibodies targeting ATGL, HSL, PLIN2 and PLIN5. LD were stained using BODIPY 493/503. Images were obtained using confocal immunofluorescence microscopy and object based colocalisation analyses were performed. Following exercise, HSL colocalisation to LD increased (P<0.05), and was significantly larger to PLIN5+LD (+53%) than to PLIN5-LD (+34%) (P<0.05), while the increases in HSL colocalisation to PLIN2+LD (+16%) and PLIN2-LD (+28%) were not significantly different. Following exercise the fraction of LD colocalised with ATGL (0.53 ± 0.04) did not significantly change (P<0.05) and was not affected by PLIN association to the LD. This study presents the first evidence of exercise-induced HSL redistribution to LD in human skeletal muscle and identifies PLIN5 as a facilitator of this mechanism.

Abbreviations: ATGL, Adipose Triglyceride Lipase; HSL, Hormone-Sensitive Lipase; DAG, Diacyglycerol; IMTG, Intramuscular Triglyceride; LD, Lipid Droplet; PLIN2, Perilipin-2; PLIN5, Perilipin-5.

Introduction

Intramuscular triglyceride (IMTG) stores provide a readily available source of energy during moderate-intensity exercise in healthy individuals. IMTG are stored within lipid droplets (LD) which are located in close proximity to mitochondria (Shaw *et al.*, 2008), which is believed to enable fatty acids (FA) liberated from IMTG to be efficiently shuttled to mitochondria to produce energy. Previously there was some debate as to whether IMTG was used during exercise because the presence of extramyocellular lipid deposits in muscle samples confounded measures of net changes in IMTG content in response to exercise (Watt *et al.*, 2002). Recent developments in confocal immunofluorescence microscopy have enabled the exclusion of extramyocellular lipid deposits and also permit fibre type-specific analyses to be performed. Using this approach, it is now well-established that IMTG stores are preferentially used from type I fibres in endurance-trained individuals during moderate-intensity exercise (van Loon *et al.*, 2003a; Shepherd *et al.*, 2013).

Hormone sensitive lipase (HSL) was previously believed to be the only rate-limiting enzyme responsible for triacylglycerol (TAG) lipolysis (Zechner *et al.*, 2009). However, it was shown that mice deficient in HSL accumulated diacylglycerol (DAG) in muscle and other tissues in response to fasting (Haemmerle *et al.*, 2002), suggesting that other lipases must exist. Adipose triglyceride lipase (ATGL) was subsequently identified as a novel lipase which preferentially hydrolyses TAG (Zimmermann *et*

al., 2004). Moreover, overexpression of ATGL in human primary myotubes results in reduced TAG content and increased FA release and oxidation (Badin *et al.*, 2011), whilst ATGL-KO mice accumulate TAG in skeletal muscle (Haemmerle *et al.*, 2006). A pertinent role for ATGL in IMTG hydrolysis stems from the finding that IMTG breakdown still occurs in electrically stimulated rat muscle following acute pharmacological inhibition of HSL or in muscle of HSL-KO mice (Alsted *et al.*, 2013). Conversely, impairment of IMTG lipolysis during exercise in mice with muscle specific deletion of ATGL was not profound enough to impact on submaximal or maximal exercise performance which may be due to a compensatory increase in HSL mediated TAG hydrolysis (Dube *et al.*, 2015). Together these data suggest that both ATGL and HSL mediate IMTG hydrolysis and both can compensate functionally when the other is absent. Muscle TAG and DAG accumulate in ATGL-KO and HSL-KO mice respectively (Haemmerle *et al.*, 2002; Haemmerle *et al.*, 2006). This, in addition to HSL having a higher specificity for DAG as a substrate in comparison to TAG (Fredrikson *et al.*, 1981), has led to the suggestion that ATGL and HSL hydrolyse IMTG in a sequential process in skeletal muscle. Importantly, ATGL and HSL together account for ~98% of contraction-induced TAG lipase activity in rat skeletal muscle (Alsted *et al.*, 2013).

HSL activity in skeletal muscle is increased during moderate-intensity exercise through protein phosphorylation induced by contraction and adrenergic signalling mechanisms (Watt *et al.*, 2003; Watt *et al.*, 2006). In addition to regulation of HSL via phosphorylation, Prats et al. (2006) elegantly demonstrated using confocal immunofluorescence microscopy that HSL translocates to LD in rat skeletal muscle *ex vivo* following stimulation with adrenaline or during electrically-induced muscle contractions. Additional examination using immunogold transmission electron microscopy on single rat muscle fibres also generated images evidencing HSL accumulation beneath the LD phospholipid monolayer suggesting that once HSL translocates to the LD it subsequently penetrates the phospholipid monolayer to access IMTG (Prats *et al.*, 2006). Moreover, in this study the colocalisation of HSL to the LD-associated protein perilipin-2 (PLIN2) increased in response to both stimuli, implicating PLIN2 in the regulation of HSL translocation to the LD (Prats *et al.*, 2006). This was the first study to generate evidence of HSL translocation in response to lipolytic stimuli. It is yet to be determined, however, if a similar mechanism occurs in human skeletal muscle within an *in vivo* environment where the regulation of HSL activity is under the control of multiple regulatory signalling factors that cannot be replicated *ex vivo*.

Under resting conditions a proportion of ATGL localizes to LDs in human skeletal muscle, and this relationship is unaltered by moderate-intensity exercise (Mason *et al.*, 2014). It is therefore reasonable to postulate that ATGL is regulated on the LD surface by its co-activator protein, CGI-58 (Lass *et al.*, 2006). Indeed, electrical stimulation of rat skeletal muscle *ex vivo* augments the co-immunoprecipitation of ATGL and CGI-58 (MacPherson *et al.*, 2013). The PLIN proteins are also believed to play a key regulatory role in controlling IMTG breakdown. Notably, the only member of the PLIN protein family that can bind ATGL is PLIN5, and in cells expressing PLIN5 both ATGL and CGI-58 are recruited to the LD under basal conditions (Wang *et al.*, 2011) suggesting that PLIN5 plays an important role in determining the activity of ATGL. Although the majority of the available evidence from cell culture studies suggests that PLIN5 (and the other PLIN proteins) facilitate the storage of TAG under basal conditions (Listenberger *et al.*, 2007; Wang *et al.*, 2011; Laurens *et al.*, 2016), PLIN5 has also been shown to promote TAG hydrolysis under conditions stimulating lipolysis in cultured cells (Wang *et al.*, 2011). Furthermore, we previously reported that LD associated with PLIN2 or PLIN5 are preferentially utilised during 1 hour of moderate-intensity exercise (Shepherd *et al.*, 2012, 2013). Whether ATGL localises to those LDs with PLIN5 associated and therefore facilitate their preferential use during exercise is yet to be investigated.

Using confocal immunofluorescence microscopy we have previously developed methods to identify LD with (PLIN+ LD) or without PLIN associated (PLIN- LD) (Shepherd *et al.*, 2012, 2013). The aim of the present study was to extend these methods and investigate the localisation of the key lipolytic en-

zymes ATGL and HSL, with PLIN2 and PLIN5 associated LD under resting conditions and in response to an acute bout of exercise in trained human skeletal muscle. We hypothesised that exercise would lead to an increase in HSL colocalisation to LDs, and that these LDs would have PLIN2 or PLIN5 associated. We also hypothesised that ATGL would already be colocalised to LD and these LD would be PLIN5 associated.

Methods

Participants and ethical approval

Archived muscle samples from a prior study of our laboratory comparing the effects of sprint interval and endurance training on IMTG utilisation during exercise (Shepherd *et al.*, 2013) were utilised in the present study. Specifically, muscle samples from 8 lean, healthy male volunteers (see Table 1 for brief subject characteristics) were analysed in the present study and the informed consent provided originally covered this subsequent use. The study was approved (09/H1202/99) by the Black Country NHS research ethics committee (West Midlands, UK) and conformed to the standards set by Declaration of Helsinki, except for registration in a database.

Experimental procedures

Following completion of 6 weeks endurance training (cycling at 65% VO_{2peak} for 40-60 mins 5 days per week; see Shepherd et al., 2013 for further details), participants rested for >72 h and consumed a controlled diet (50%, carbohydrate, 35% fat and 15% protein) matched to habitual caloric intake for 24 h prior to the experimental trial. Following an overnight fast (>10 h), participants performed 60 min cycling on a stationary ergometer at 50 ± 2% W_{max} (equating to ~59% $\dot{V}o_{2peak}$ achieved post-training intervention). Expired air was collected (5 min collection period) at 15 min intervals (t = 15, 30, 45, 60 min), using an online gas system (Oxycon Pro, Jaeger, Germany) in order to calculate rates of carbohydrate and lipid oxidation (Table 2). Additionally, heart rate was recorded every 5 min (Table 2).

Muscle biopsies were obtained from the *m. vastus lateralis* of one leg before (0 min) and immediately after exercise (60 min). The biopsied leg was randomised to avoid any bias of dominant leg. Initially local anaesthetic (1% lidocaine; B Braun, Sheffield, UK) was injected into the skin and fascia of the muscle before two small incisions were made approximately 2 cm apart. Prior to exercise, a muscle biopsy (~100 mg) was extracted from the distal incision using the Bergström needle technique (Bergström, 1975). The muscle biopsy was first dissected from any fat or connective tissue. A portion (~60mg) of muscle was immediately embedded in Tissue-Tek OCT compound (Sakura Finetek Europe, The Netherlands) and frozen in liquid nitrogen-cooled isopentane for subsequent immunohistochemical analyses. Following exercise, the second muscle biopsy was taken from the proximal incision using the method described above.

Analysis of muscle samples

Immunofluorescence staining.

Cryosections (5 µm) were cut at -25^{o}C onto ethanol-cleaned glass slides. Cryosections of both pre- and post-exercise samples from one participant were placed on a single slide to account for any variation in staining intensity between sections. Sections were fixed for 1 h in 3.7% formaldehyde, rinsed 3 x 30 s in doubly distilled water (dd H_2O) and permeabilised in 0.5% Triton X-100 for 5 min, before being washed 3 x 5 min in Phosphate Buffered Saline (PBS, 137mM sodium chloride, 3 mM potassium chloride, 8 mM sodium phosphate dibasic and 3mM potassium phosphate monobasic, pH of 7.4). Subsequently, slides were incubated with primary antibodies (overnight for HSL analysis, 1 hr for ATGL analysis) before being washed again 3 x 5 min in PBS. Sections were then incubated with complementary secondary fluorescence-conjugated antibodies for 30 min, followed by a further 3 x 5 min PBS washes. To visualise LD, sections were incubated with BODIPY 493/503 (Invitrogen, Pais-

ley, UK, D3922, dilution 1:50) for 20 min followed by a further 1 x 5 min PBS wash. After the final wash, coverslips were mounted with Vectashield (H-1000, Vector Laboratories, Burlingame, CA, USA) and sealed.

HSL and ATGL visualisation was achieved using rabbit polyclonal anti-HSL (Abcam, Cambridge, UK, ab 63492, dilution 1:50) or rabbit polyclonal anti-ATGL (Abcam, Cambridge, UK, Ab109251, dilution 1:50) respectively, followed by application of Alexa Fluor goat anti-rabbit IgG 546 secondary antibody (Invitrogen, Paisley, UK, A-11035, dilution 1:100). PLIN2 was visualised with mouse monoclonal anti-adipophilin (PLIN2) (American Research Products, MA, USA, GP40, dilution 1:50) and Alexa Fluor goat anti-mouse IgG_1 633 secondary antibody (Invitrogen, Paisley, UK, A-21126, dilution 1:100). PLIN5 was visualised with guinea pig polyclonal anti-OXPAT (PLIN5) (Progen Biotechnik, Germany, GP31, dilution 1:100) and Alexa Fluor goat anti-guinea pig IgG 633 secondary antibody (Invitrogen, Paisley, UK, A-21105, dilution 1:100). Initially, sections were co-stained for HSL and LD to investigate HSL localisation to LD. HSL and LD were then co-stained with either PLIN2 or PLIN5 in order to determine HSL localisation to LD either associated (PLIN+ LDs) or not associated with each PLIN protein (PLIN- LDs). This process was then repeated with ATGL and LD being co-stained with either PLIN2 or PLIN5 to establish ATGL localisation to LD either associated (PLIN+ LDs) or not associated with each PLIN protein (PLIN- LDs). As described previously (Shepherd *et al.*, 2012, 2013; Strauss *et al.*, 2016; Shepherd *et al.*, 2017), before any colocalisation analysis was undertaken controls were included to confirm absence of 1) bleed through of fluorophores in opposing channels when single staining was performed, 2) non-specific secondary antibody binding, and 3) sample autofluorescence.

Image capture, processing and data analysis

An inverted confocal microscope (Zeiss LSM710; Oberkochen, Germany) was used to obtain digital images of cross-sectionally orientated muscle sections. An argon laser was used to excite the Alexa Fluor 488 fluorophore whilst a helium-neon laser excited the Alexa Fluor 546 and 633 fluorophores. Images were initially acquired with a 40x 0.7 NA oil immersion objective to examine the cellular distribution of HSL and LDs. The same system was used but with a 16x digital magnification to acquire images that were used to investigate HSL and LD colocalisation. A more powerful oil immersion objective of 63x 1.4 NA combined with 16x digital magnification was then used to identify LD that were coated with PLIN and assess the localisation of HSL to these LD. ATGL appeared punctate and dispersed throughout the cell and to capture its distribution more representatively, images were acquired using the 63X 1.4 NA objective at a wider 8x digital magnification. We were unable to stain for and identify type I fibres during the immunohistochemical analysis in the current study due to limitations on the number of fluorophores that could be used simultaneously. Instead, only muscle fibres that had the highest lipid content were imaged. Type I fibres typically have a high IMTG content alongside a large oxidative capacity (Shaw *et al.*, 2008; Shepherd *et al.*, 2013), and we have previously shown that IMTG utilisation during exercise occurs specifically in type I fibres (Shepherd *et al.*, 2012, 2013). Results from our previous study also clearly demonstrated that 'in comparison to type IIa fibres, type I fibres had 3-4 fold and 2-3 fold greater IMTG stores pre and post-exercise, respectively (Shepherd *et al.*, 2013). Therefore, by selecting fibres with the highest lipid content we are assuming those fibres would also have the highest oxidative capacity and rates of IMTG utilisation during exercise. We expect that this approach would consequently detect changes in lipase association with LD if they existed. For each participant, images were obtained of pre-exercise muscle fibres (n=15) and post-exercise muscle fibres (n=15) with the central region of the fibre imaged for each staining combination. Due to insufficient sample being available, ATGL immunohistochemical analysis was only performed on 7 participants.

Image analysis was undertaken using Image-Pro Plus 5.1 software (Media Cybernetics, Bethesda, MD, USA). For colocalisation analysis, an intensity threshold was selected to denote the positive signal for HSL or ATGL, LD (Fig. 1) and PLIN2 or PLIN5. These thresholds were then used to produce binary images of HSL or ATGL, LD, PLIN2 or PLIN5 that were subsequently used for colocalisation

analysis (Fig. 1). A co-localisation map displaying the merged images was generated, and the overlapping regions extracted to a separate image. Initially colocalisation between LD and HSL was measured by expressing the total number of extracted objects as a proportion of the total number of LDs. To determine HSL colocalisation to LDs with or without PLIN associated the following analysis was conducted. LD that colocalised with PLIN were first characterised as PLIN+ and PLIN- LDs (Shepherd *et al.*, 2013). The number of PLIN+ LDs and PLIN- LDs that overlapped with HSL was then counted per image pre and post-exercise. The number of PLIN+ and PLIN- LDs colocalised with HSL was then expressed relative to area, thereby enabling us to quantify the density of each LD subgroup to be colocalised with HSL. HSL colocalisation to PLIN2 or PLIN5 was also quantified irrespective of LD presence. The same process was then repeated for ATGL instead of HSL. Additional analysis on the size and number of HSL or ATGL objects per image was conducted to generate a clear understanding of HSL and ATGL distribution pre- and post-exercise.

Statistics

All data are expressed as means ± SEM. Significance was set at $P < 0.05$. A student's paired *t* test was used to measure differences from pre- to post-exercise in variables relating to HSL or ATGL colocalisation to LD. A Wilcoxon signed rank test was used to measure the differences in HSL average area from pre- to post-exercise due to non-normally distributed data. A two-way within-subjects ANOVA was used to measure the differences in HSL colocalisation with LD pre and post-exercise, where within subjects factors were identified as *'time'* (pre vs post-exercise) and *'HSL-colocalisation'* (HSL+ LD *vs.* HSL- LD). A two-way within-subjects ANOVA was also used to measure the differences in HSL or ATGL colocalisation to PLIN+ and PLIN- LDs, pre- and post-exercise. Here, the within-subject factors were identified as *'time'* (pre- *vs.* post-exercise) and *'PLIN-association'* (PLIN+ LD *vs*. PLIN- LD). Significant main effects or interaction effects were assessed using Bonferroni adjustment *post hoc* analysis.

Results

Substrate utilisation

The RER remained stable during the 60 min of cycling at 59 ± 2% $\dot{V}o_{2peak}$. Fat oxidation rates increased throughout the exercise bout and averaged 45 ± 3% of total substrate oxidation (Table 2).

Increased HSL localisation to LDs following exercise

Images of immunofluorescence staining of HSL showed large storage clusters dispersed throughout the cell (Fig. 2A). Fibres that exhibited a high lipid content were selected and images of HSL and BODIPY 493/503 were obtained from the central part of each fibre at 16x digital magnification. Using this approach, it became clear that in response to exercise there was a shift in the distribution of HSL from large clusters to a greater number of smaller, discrete clusters (representative images shown in Fig. 2B). Accordingly, there was a significant increase in the number of HSL clusters from pre (0.0919 ± 0.0068 μm^{-2}) to post-exercise (0.1250 ± 0.0082 $\mu m^{-}2$; $P = 0.001$) whilst the size of each HSL cluster significantly decreased from pre (*Mdn* = 44.20) to post-exercise (*Mdn* = 38.04; $Z = 2.4$; $P = 0.025$). Importantly, HSL protein content as measured by fluorescence intensity did not change from pre- (39 ± 3 AU) to post-exercise (42 ± 4 AU; $P = 0.107$). The fraction of LD colocalised with HSL clusters significantly increased (19%; $P = 0.014$; Fig. 3A). At baseline, there were significantly more LD that were colocalised to HSL than LD without HSL colocalisation ($P = 0.033$; Fig. 3B). Following exercise there was a significant interaction effect ($P = 0.014$), the number of LD that were colocalised to HSL significantly increased from pre to post-exercise (+21%, $P = 0.014$) whereas the number of LD without HSL colocalisation showed a trend towards a decrease pre to post-exercise (- 22%, $P = 0.063$; Fig. 3B).

ATGL and LD analysis

Immunofluorescence staining of ATGL showed a distinct punctate pattern throughout the cytosol which was unaltered following exercise (Fig. 4). ATGL protein content as measured by fluorescence intensity was not significantly different from pre (7 ± 1 AU) to post-exercise (8 ± 1 AU; $P = 0.354$). The average area of each ATGL object per image was unchanged from pre (40.61 ± 8.72 μm^{-2}) to post-exercise (41.35 ± 9.66 μm^{-2}, $P = 0.733$). The number of ATGL objects was also unchanged from pre (0.044 ± 0.004 μm^{-2}) to post-exercise (0.044 ± 0.002 μm^{-2}; $P = 0.925$). The fraction of LD colocalised with ATGL was not significant differently from pre (0.53 ± 0.04) to post-exercise (0.43 ± 0.05, $P = 0.069$). As such, the number of LD colocalised with ATGL was not different from pre (0.0331 ± 0.0035 μm^{-2}) to post-exercise (0.0285 ± 0.0040 μm^{-2}; $P = 0.326$). Similarly, the number of LD without ATGL colocalisation was not different from pre (0.0304 ± 0.0028 μm^{-2}) to post-exercise (0.0350 ± 0.0021 μm^{-2}; $P = 0.253$).

Relationship between HSL, PLIN2 or PLIN5 and LD

To quantify colocalisation between HSL and PLIN2+ LD or PLIN2- LD, images of HSL, PLIN2 and LD were acquired pre and post-exercise at 16x magnification using a 63x 1.4 NA objective (Fig. 5A). This process was then repeated for HSL, PLIN5 and LD (Fig. 5B). The number of HSL objects colocalised to PLIN2 increased from pre (0.0688 ± 0.0030 μm^{-2}) to post-exercise (0.0773 ± 0.0020 μm^{-2}; $P = 0.049$). However, not all LDs have PLIN2 bound to them, and therefore we investigated the colocalisation of HSL with PLIN2+ and PLIN2- LDs. Pre-exercise, the number of PLIN2+ LD colocalised to HSL was greater (0.0565 ± 0.0043 μm^{2}) than the number of PLIN2- LD not colocalised with HSL (0.0205 ± 0.0019 μm^{-2}; $P < 0.001$; Fig 6A). Exercise led to an increase in HSL colocalisation to both PLIN2+ LD (+16%) and PLIN2- LD (+28%; Fig. 6A, $P = 0.047$) post-exercise. There was however, no interaction effect for exercise and PLIN2 presence on the LD ($P = 0.611$).

The number of HSL objects colocalised to PLIN5 also increased from pre (0.0573 ± 0.0043 μm^{-2}) to post-exercise (0.0772 ± 0.0056 μm^{-2}; $P = 0.002$). Pre-exercise, the number of PLIN5+ LD colocalised with HSL was greater (0.0406 ± 0.0043 μm^{-2}) compared to the number of PLIN5- LD without HSL colocalisation (0.0149 ± 0.0015 μm^{-2}; $P = 0.001$; Fig. 6B). There was a main effect for exercise on HSL colocalisation to LD ($P < 0.001$; Fig. 6B), such that HSL colocalisation to LD increased. Moreover, there was a significant interaction effect for exercise and PLIN5 presence on the LD. The increase in HSL colocalisation to PLIN5+ LD (+53%) was greater than the increase to PLIN5- LD (+34%; $P = 0.006$; Fig. 6B).

Relationship between ATGL, PLIN2 or PLIN5 and LD

To quantify colocalisation between ATGL and PLIN2+ LD or PLIN2- LD, 16x magnification images on a 63x 1.4 NA objective were acquired pre- and post-exercise of ATGL, PLIN2 and LD (Fig. 4B). This process was then repeated for ATGL, PLIN5 and LD. Pre-exercise, there was greater ATGL colocalised to PLIN2+ LD (0.0224 ± 0.0029 μm^{-2}) compared to PLIN2- LD (0.0057 ± 0.001 μm^{-2}, $P < 0.001$; Fig. 7A) and this was unaltered with exercise ($P = 0.187$). Pre-exercise, more ATGL was colocalised to PLIN5+ LD (0.0222 ± 0.0017 μm^{-2}) compared to PLIN5- LD (0.0109 ± 0.0019 μm^{-2}, $P < 0.001$; Fig. 7B) and this was also not altered with exercise ($P = 0.287$). There was no significant difference in the amount of ATGL colocalised to PLIN2 from pre (0.037 ± 0.0033 μm^{-2}) to post- exercise (0.037 ± 0.0023 μm^{-2}; $P = 0.985$). There was also no significant difference in the amount of ATGL colocalised to PLIN5 from pre (0.0305 ± 0.0018 μm^{-2}) to post-exercise (0.0311 ± 0.0023; $P = 0.877$).

Discussion

This study examined the localisation of the two key lipases in human skeletal muscle, ATGL and HSL, with LDs and the associated PLIN proteins at rest and in response to moderate-intensity exercise.

The major novel observation is that HSL redistributes to LD in human skeletal muscle following 1 h moderate-intensity cycling exercise, with HSL preferentially translocating to LDs with PLIN5 associated. Furthermore, we confirm for the first time that ATGL was colocalised more to PLIN5+ LD in comparison to PLIN5- LD in agreement with our hypothesis. Additionally, the data shows that ATGL is also colocalised more to PLIN2+ LD in comparison to PLIN2- LD and the distribution of ATGL does not alter during the exercise bout. Together, these data demonstrate different distribution patterns of key lipases and their localisation to LD-associated PLIN proteins in skeletal muscle, which may be important in the regulation of IMTG utilisation during moderate-intensity exercise.

In the basal state HSL was observed as large storage clusters throughout the cell, whereas after exercise HSL was visualised as a greater number of smaller, discrete clusters typically centred on LD (Fig. 2B). As a result, we observed an increase in the fraction of LD colocalising with HSL from pre to post-exercise, demonstrating HSL redistributes to LD in response to exercise in human skeletal muscle. A number of studies in cultured adipocytes have demonstrated that HSL translocates from the cytosol to LD in response to lipolytic stimuli (Su *et al.*, 2003; Sztalryd *et al.*, 2003; Wang *et al.*, 2009), whereas studies investigating the localisation of HSL in skeletal muscle are limited. Most notably, Prats et al. (2006) in line with our findings using confocal immunofluorescence microscopy and isolated rat skeletal muscle fibres observed that HSL in the basal state was accumulating either as storage clusters or colocalising with LD, whilst ex vivo electrical or adrenaline stimulation increased the translocation of HSL to LD. In addition transmission electron microscopy using immunogold labelled HSL antibodies was used in the study of Prats et al. (2006) to show that the HSL translocation led to HSL passing the phospholipid monolayer of the LD into the TAG core (Prats *et al.*, 2006) allowing HSL (the enzyme) greater access to IMTG (the substrate). The *ex vivo* protocol adopted by Prats et al. (2006) elegantly eliminates the interference of plasma-derived FA on substrate use and IMTG synthesis allowing for IMTG hydrolysis to be studied in isolation. We now extend these findings to demonstrate that HSL redistribution occurs in human skeletal muscle in response to moderate-intensity exercise *in vivo*.

Overall we observed an increase in HSL colocalisation to PLIN2 and PLIN5 following exercise. This finding is in agreement with Prats et al. (2006) who demonstrated an increased colocalisation of HSL with PLIN2, but did not investigate PLIN5. In addition, by staining HSL, LD and either PLIN2 or PLIN5, we were able to determine specific colocalisation between HSL and different sub-groups of LD (PLIN2+ LD and PLIN2- LD or PLIN5+ LD and PLIN5- LD). The most important and novel finding of the present study was that HSL preferentially redistributed to LDs with associated PLIN5. Although PLIN5 is implicated in protecting intracellular TAG stores from hydrolysis under basal conditions (Wang *et al.*, 2011; Laurens *et al.*, 2016), evidence is accumulating that PLIN5 also facilitates TAG breakdown when energy demand increases. PLIN5 is phosphorylated in response to PKA stimulation leading to TAG hydrolysis in cultured cells (Wang *et al.*, 2011). In addition, we have previously shown that LDs with PLIN5 associated are preferentially used during a bout of moderate-intensity exercise in lean, healthy individuals (Shepherd *et al.*, 2013). We now propose that PLIN5+ LDs are targeted for breakdown during exercise because PLIN5 facilitates the interaction of HSL with the TGs stored in the LD core.

Immunofluorescence staining of ATGL displayed a punctate pattern throughout the cytosol which was not altered in response to moderate-intensity exercise (Fig. 4). At baseline the fraction of LD colocalising with ATGL was ~0.53 and this was not altered following exercise. Mason et al., (2014) recently reported no significant changes in the percentage of ATGL colocalising with LD (stained using Oil Red O) in human skeletal muscle of recreationally active males following moderate-intensity exercise. Together these results suggest that a proportion of LD already is colocalising with ATGL under basal conditions and that the activity of ATGL is instead regulated by its co-activator CGI-58. In line with this suggestion, studies in cultured COS-7 cells have shown that overexpression of GGI-58 led to an increase in ATGL activity (Lass *et al.*, 2006). The fraction of LD colocalising with ATGL showed a trend

towards a decrease after exercise, which is likely explained by a decrease in LD number post-exercise (Shepherd *et al.*, 2013). Interestingly the results show there is a substantial fraction of LD (~0.47) that do not have any colocalisation with ATGL. As HSL acts both on TAG and DAG (Lass *et al.*, 2011) it is plausible that LD not colocalised with ATGL are instead subject to HSL-mediated hydrolysis.

Evidence from cultured cells suggests PLIN5 recruits and binds ATGL and CGI-58 at the LD surface under basal conditions but releases ATGL and CGI-58 following PKA induced phosphorylation (Granneman *et al.*, 2011; Wang *et al.*, 2011). The release of ATGL and CGI-58 from PLIN5 allows ATGL to bind to its co-activator CGI-58 to increase ATGL activity (Granneman *et al.*, 2011; Wang *et al.*, 2011). In the current study at baseline, ATGL colocalisation was higher to PLIN2+ LD and PLIN5+ LD in comparison to PLIN2- LD and PLIN5- LD respectively (Fig. 8). As ATGL distribution did not change during exercise, the amount of ATGL colocalised with PLIN2+ LD and PLIN5+ LD was also not altered after the exercise bout. There was also no change in ATGL colocalisation with PLIN2 or PLIN5 irrespective of LD presence following exercise. In line with our findings, MacPherson et al. (2013) also reported that PLIN2 and PLIN5 both co-immunoprecipitated with ATGL under basal conditions, but this did not increase in response to lipolytic stimuli (adrenaline, contraction or both) in rat skeletal muscle. Our data therefore suggests that PLIN2 and PLIN5 may support the positioning of ATGL to LD during fasted, non-exercised conditions. Immunogold labelling of HSL with transmission electron microscopy has confirmed that HSL penetrates the phospholipid monolayer of the LD to access IMTG in response to epinephrine or electrical stimulation in isolated rat skeletal muscle (Prats *et al.*, 2006). Whether PLIN2 or PLIN5 localises ATGL to the outside of the LD phospholipid monolayer during basal conditions but then releases ATGL so it can penetrate the phospholipid monolayer and access IMTG stores clearly warrants further investigation but can only accurately deciphered using immunogold transmission electron microscopy.

IMTG utilisation during 60 min of moderate-intensity cycling exercise in these muscle samples was quantified previously, where it was confirmed that IMTG content decreased from pre to post-exercise (-43 ± 5%) in type I fibres only (Shepherd *et al.*, 2013). Due to constraints with the number of fluorophores that could be used simultaneously we were unable to stain and identify type I fibres as part of the analysis in this study. Instead, fibres with the highest lipid content were selected for analysis. Type I fibres are characterised by high mitochondrial content and elevated IMTG stores (Shaw *et al.*, 2008; Shepherd *et al.*, 2013). It is well documented that IMTG utilisation is strongly associated with pre-exercise IMTG content (van Loon *et al.*, 2003a; van Loon *et al.*, 2003b) and it is therefore likely that the fibres selected in the current study also exhibited net IMTG breakdown. Moreover, despite being unable to identify fibre type in the current study we can conclude that redistribution of HSL occurs in fibres that have a high LD content.

By extending our validated immunofluorescence microscopy techniques, we have been able to generate further insight into the role of the PLIN proteins in the regulation of lipolysis in skeletal muscle during endurance exercise. Our assays, however, only permit the analysis of ATGL or HSL colocalisation with LDs with a single PLIN protein. It is possible, therefore, that PLIN2+ LD or PLIN2- LD may have PLIN5 associated and similarly PLIN5+ LD and PLIN5- LD may have PLIN2 associated. Nevertheless, the results indicate that whilst there were similar increases in HSL colocalisation to PLIN2+ LD and PLIN2- LD post-exercise, there was a significantly greater increase in HSL colocalisation to PLIN5+ LD in comparison to PLIN5- LD after the exercise bout. It is also possible, that PLIN5 was also present on the surface of PLIN2+ LD or PLIN2- LDs colocalised with ATGL. Despite this limitation we can still conclude that ATGL was present on PLIN5- LDs and therefore PLIN5 is not a prerequisite for ATGL colocalisation to the LD.

In conclusion, this study has generated novel evidence that HSL redistributes to LD in skeletal muscle of endurance-trained men in response to moderate-intensity exercise, whereas ATGL colocalisation

with LDs is unaltered by exercise. Furthermore, this is the first study to demonstrate that HSL preferentially redistributes to PLIN5+ LDs following moderate intensity exercise, demonstrating a novel mechanism by which PLIN5 regulates HSL recruitment to LD which could aid in subsequent IMTG utilisation during exercise.

Additional Information

Competing interest
The authors declare that they have no competing interests.

Author Contributions
KLW, SOS and JAS were responsible for the conception and design of the experiments. KLW, SOS and JAS were responsible for the collection and analysis of data. KLW, SOS, AJMW and JAS were responsible for interpretation of the data and drafting and revisions of the manuscript. All authors approved of the final version of the manuscript, and agree to be accountable for all aspects of the work in ensuring that questions related to the accuracy or integrity of any part of the work are appropriately investigated and resolved, and all persons designated as authors qualify for authorship, and all those who qualify for authorship are listed.

Funding
KLW is in receipt of a PhD scholarship from LJMU.

Acknowledgements
The muscle samples used in this study were obtained from a previous study. The authors would like to thank Dr Christopher Shaw and Dr Matthew Cocks in their assistance in collecting the original samples.

References

Alsted TJ, Ploug T, Prats C, Serup AK, Hoeg L, Schjerling P, Holm C, Zimmermann R, Fledelius C, Galbo H & Kiens B. (2013). Contraction-induced lipolysis is not impaired by inhibition of hormone-sensitive lipase in skeletal muscle. *J Physiol* **591,** 5141-5155.

Badin PM, Louche K, Mairal A, Liebisch G, Schmitz G, Rustan AC, Smith SR, Langin D & Moro C. (2011). Altered skeletal muscle lipase expression and activity contribute to insulin resistance in humans. *Diabetes* **60,** 1734-1742.

Bergström J. (1975). Percutaneous needle biopsy of skeletal muscle in physiological and clinical research. *Scand J Clin Lab Invest* **35,** 609-616.

Dube JJ, Sitnick MT, Schoiswohl G, Wills RC, Basantani MK, Cai L, Pulinilkunnil T & Kershaw EE. (2015). Adipose triglyceride lipase deletion from adipocytes, but not skeletal myocytes, impairs acute exercise performance in mice. *Am J Physiol Endocrinol Metab* **308,** E879-890.

Fredrikson G, Stralfors P, Nilsson NO & Belfrage P. (1981). Hormone-sensitive lipase from adipose tissue of rat. *Methods Enzymol* **71 Pt C,** 636-646.

Granneman JG, Moore HP, Mottillo EP, Zhu Z & Zhou L. (2011). Interactions of perilipin-5 (Plin5) with adipose triglyceride lipase. *J Biol Chem* **286,** 5126-5135.

Haemmerle G, Lass A, Zimmermann R, Gorkiewicz G, Meyer C, Rozman J, Heldmaier G, Maier R, Theussl C, Eder S, Kratky D, Wagner EF, Klingenspor M, Hoefler G & Zechner R. (2006). Defective lipolysis and altered energy metabolism in mice lacking adipose triglyceride lipase. *Science* **312,** 734-737.

Haemmerle G, Zimmermann R, Hayn M, Theussl C, Waeg G, Wagner E, Sattler W, Magin TM, Wagner EF & Zechner R. (2002). Hormone-sensitive lipase deficiency in mice causes diglyceride accumulation in adipose tissue, muscle, and testis. *J Biol Chem* **277,** 4806-4815.

Lass A, Zimmermann R, Haemmerle G, Riederer M, Schoiswohl G, Schweiger M, Kienesberger P, Strauss JG, Gorkiewicz G & Zechner R. (2006). Adipose triglyceride lipase-mediated lipolysis of cellular fat stores is activated by CGI-58 and defective in Chanarin-Dorfman Syndrome. *Cell Metab* **3,** 309-319.

Lass A, Zimmermann R, Oberer M & Zechner R. (2011). Lipolysis - a highly regulated multi-enzyme complex mediates the catabolism of cellular fat stores. *Prog Lipid Res* **50,** 14-27.

Laurens C, Bourlier V, Mairal A, Louche K, Badin PM, Mouisel E, Montagner A, Marette A, Tremblay A, Weisnagel JS, Guillou H, Langin D, Joanisse DR & Moro C. (2016). Perilipin 5 fine-tunes lipid oxidation to metabolic demand and protects against lipotoxicity in skeletal muscle. *Sci Rep* **6,** 38310.

Listenberger LL, Ostermeyer-Fay AG, Goldberg EB, Brown WJ & Brown DA. (2007). Adipocyte differentiation-related protein reduces the lipid droplet association of adipose triglyceride lipase and slows triacylglycerol turnover. *J Lipid Res* **48,** 2751-2761.

MacPherson RE, Ramos SV, Vandenboom R, Roy BD & Peters SJ. (2013). Skeletal muscle PLIN proteins, ATGL and CGI-58, interactions at rest and following stimulated contraction. *Am J Physiol Regul Integr Comp Physiol* **304,** R644-650.

Mason RR, Meex RC, Russell AP, Canny BJ & Watt MJ. (2014). Cellular localization and associations of the major lipolytic proteins in human skeletal muscle at rest and during exercise. *PLoS One* **9,** e103062.

Prats C, Donsmark M, Qvortrup K, Londos C, Sztalryd C, Holm C, Galbo H & Ploug T. (2006). Decrease in intramuscular lipid droplets and translocation of HSL in response to muscle contraction and epinephrine. *J Lipid Res* **47,** 2392-2399.

Shaw CS, Jones DA & Wagenmakers AJ. (2008). Network distribution of mitochondria and lipid droplets in human muscle fibres. *Histochem Cell Biol* **129,** 65-72.

Shepherd SO, Cocks M, Tipton KD, Ranasinghe AM, Barker TA, Burniston JG, Wagenmakers AJ & Shaw CS. (2012). Preferential utilization of perilipin 2-associated intramuscular triglycerides during 1 h of moderate-intensity endurance-type exercise. *Exp Physiol* **97,** 970-980.

Shepherd SO, Cocks M, Tipton KD, Ranasinghe AM, Barker TA, Burniston JG, Wagenmakers AJ & Shaw CS. (2013). Sprint interval and traditional endurance training increase net intramuscular triglyceride breakdown and expression of perilipin 2 and 5. *J Physiol* **591,** 657-675.

Shepherd SO, Strauss JA, Wang Q, Dube JJ, Goodpaster B, Mashek DG & Chow LS. (2017). Training alters the distribution of perilipin proteins in muscle following acute free fatty acid exposure. *J Physiol* **595,** 5587-5601.

Strauss JA, Shaw CS, Bradley H, Wilson OJ, Dorval T, Pilling J & Wagenmakers AJ. (2016). Immunofluorescence microscopy of SNAP23 in human skeletal muscle reveals colocalization with plasma membrane, lipid droplets, and mitochondria. *Physiol Rep* **4**.

Su CL, Sztalryd C, Contreras JA, Holm C, Kimmel AR & Londos C. (2003). Mutational analysis of the hormone-sensitive lipase translocation reaction in adipocytes. *J Biol Chem* **278,** 43615-43619.

Sztalryd C, Xu G, Dorward H, Tansey JT, Contreras JA, Kimmel AR & Londos C. (2003). Perilipin A is essential for the translocation of hormone-sensitive lipase during lipolytic activation. *J Cell Biol* **161,** 1093-1103.

van Loon LJ, Koopman R, Stegen JH, Wagenmakers AJ, Keizer HA & Saris WH. (2003a). Intramyocellular lipids form an important substrate source during

moderate intensity exercise in endurance-trained males in a fasted state. *J Physiol* **553,** 611-625.

van Loon LJ, Schrauwen-Hinderling VB, Koopman R, Wagenmakers AJ, Hesselink MK, Schaart G, Kooi ME & Saris WH. (2003b). Influence of prolonged endurance cycling and recovery diet on intramuscular triglyceride content in trained males. *Am J Physiol Endocrinol Metab* **285,** E804-811.

Wang H, Bell M, Sreenivasan U, Hu H, Liu J, Dalen K, Londos C, Yamaguchi T, Rizzo MA, Coleman R, Gong D, Brasaemle D & Sztalryd C. (2011). Unique regulation of adipose triglyceride lipase (ATGL) by perilipin 5, a lipid droplet-associated protein. *J Biol Chem* **286,** 15707-15715.

Wang H, Hu L, Dalen K, Dorward H, Marcinkiewicz A, Russell D, Gong D, Londos C, Yamaguchi T, Holm C, Rizzo MA, Brasaemle D & Sztalryd C. (2009). Activation of hormone-sensitive lipase requires two steps, protein phosphorylation and binding to the PAT-1 domain of lipid droplet coat proteins. *J Biol Chem* **284,** 32116-32125.

Watt MJ, Heigenhauser GJ & Spriet LL. (2002). Intramuscular triacylglycerol utilization in human skeletal muscle during exercise: is there a controversy? *J Appl Physiol (1985)* **93,** 1185-1195.

Watt MJ, Holmes AG, Pinnamaneni SK, Garnham AP, Steinberg GR, Kemp BE & Febbraio MA. (2006). Regulation of HSL serine phosphorylation in skeletal muscle and adipose tissue. *Am J Physiol Endocrinol Metab* **290,** E500-508.

Watt MJ, Stellingwerff T, Heigenhauser GJ & Spriet LL. (2003). Effects of plasma adrenaline on hormone-sensitive lipase at rest and during moderate exercise in human skeletal muscle. *J Physiol* **550,** 325-332.

Zechner R, Kienesberger PC, Haemmerle G, Zimmermann R & Lass A. (2009). Adipose triglyceride lipase and the lipolytic catabolism of cellular fat stores. *J Lipid Res* **50,** 3-21.

Zimmermann R, Strauss JG, Haemmerle G, Schoiswohl G, Birner-Gruenberger R, Riederer M, Lass A, Neuberger G, Eisenhaber F, Hermetter A & Zechner R. (2004). Fat mobilization in adipose tissue is promoted by adipose triglyceride lipase. *Science* **306,** 1383-1386.

TABLE 1. Subject characteristics	
Age (years)	21 ± 1
Height (m)	1.77 ± 0.03
Body mass (kg)	70.8 ± 4.5
BMI (kg m^{-2})	22.6 ± 1.2
$\dot{V}o_{2peak}$ (l min^{-1})	3.40 ± 0.38
$\dot{V}o_{2peak}$ (l min^{-1} kg^{-1})	48.2 ± 5.0
W_{max} (W)	253 ± 16
FFM (kg)	51.1 ± 2.7
FM (kg)	12.2 ± 1.9
ISI-Matsuda	4.7 ± 0.7

Figure 1. Method of colocalisation analysis.

Binary images of objects representing HSL (A) and LD (B) identified by a selected intensity threshold to signify a positive signal for HSL or LD, respectively. Colocalisation of HSL objects and LD was investigated by merging the images (C), and the extracted objects (D) represents positive colocalisation between HSL and LD. Any LD that overlapped with a HSL object was counted as colocalisation event. If the same HSL object over-lapped more than once with a LD then this was counted as a dual colocalisation event and omitted from the analysis, allowing for only one colocalisation event to be counted. The same procedure was used to obtain colocalisation analysis for ATGL objects and LD, PLIN2 or PLIN5 and LD. White bars represent 3 μm.

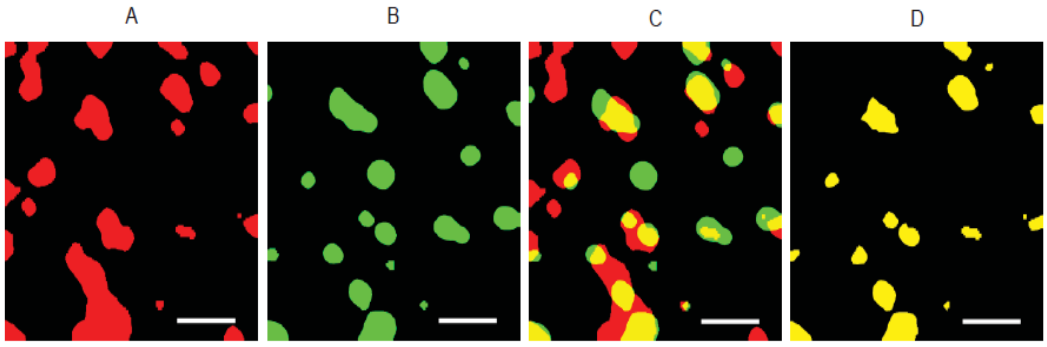

Figure 2. HSL redistributes to LD following from pre to post-exercise as visualised through confocal immunofluorescence microscopy.

Representative images of HSL and LD pre and post-exercise were initially obtained using a 40x oil objective on a confocal microscope (A). White bars represent 50 μm. LD were visualised using BODIPY 493/503 and represent IMTG stores within the cell. Muscle fibres that had the highest lipid droplet content were selected for analysis. A 16x digital magnification was then applied to the centre of these muscle fibres and images were obtained to identify and quantify distribution and colocalisation be-

tween HSL and LD (B). White bars represent 2 μm. Image B shows that in the pre-exercise state HSL appeared as large storage clusters throughout the cell, whereas post-exercise HSL was visualised as a greater number of smaller, discrete clusters centred on LDs as observed on the merged images.

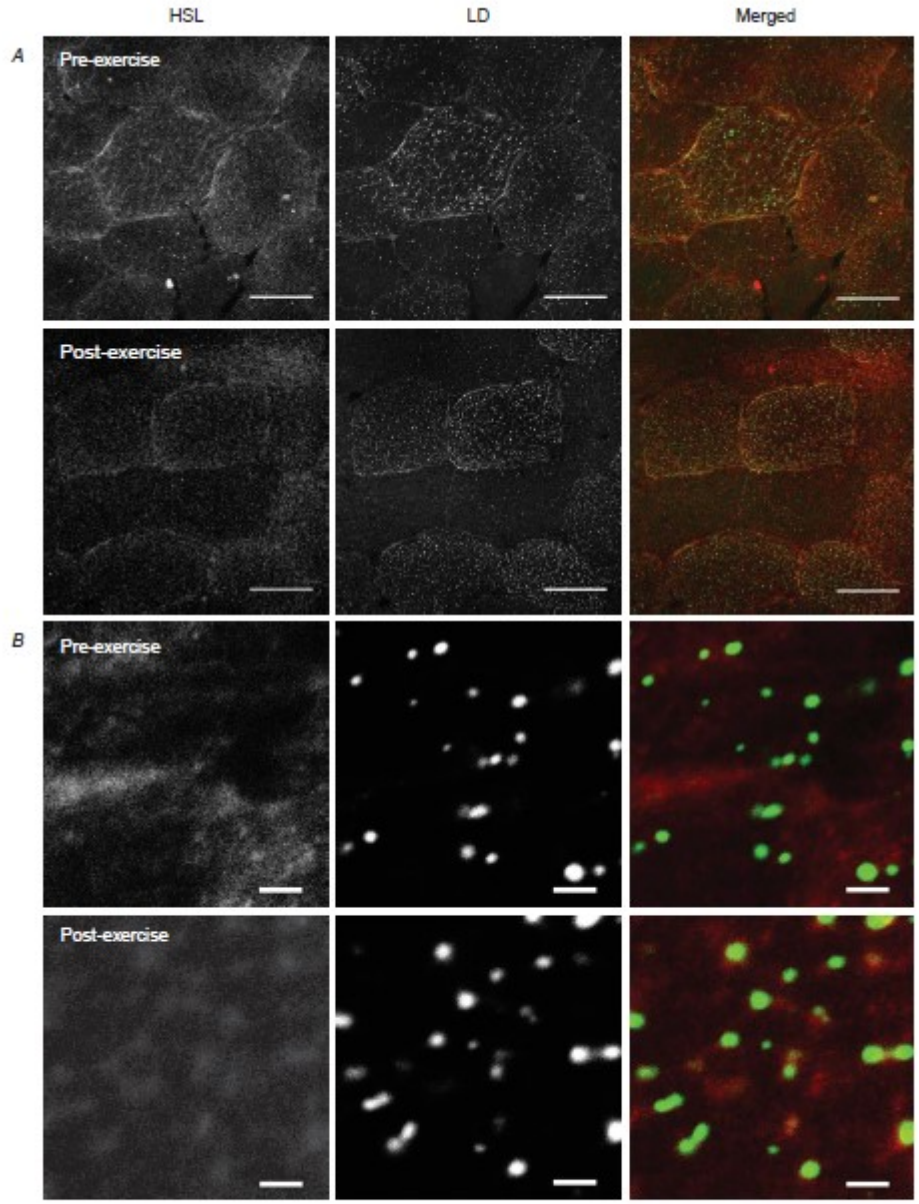

Figure 3. HSL redistributes from larger storage clusters to smaller more frequent clusters from pre to post exercise resulting in an increase in LD colocalisation to HSL.

Quantification derived from confocal immunofluorescence microscopy images. Colocalisation analysis was performed to determine the fraction of LD overlapping with HSL objects pre- and post-exercise (A). Subsequently, the number of LD colocalised with HDL (HSL+ LD) or not colocalised with HSL (HSL- LD) was calculated and compared from pre to post-exercise (B). Data collected are averages of

15 fibres per participant per time point. Values are given as means ± SEM (n = 8 per group). †Main effect for HSL colocalisation to LD (P < 0.05 *vs.* HSL- LD). ‡ Main interaction effect for HSL colocalisation to LD from pre to post-exercise (P < 0.05). Post-hoc analysis revealed an increase in HSL+ LD (* P < 0.05 *versus* pre-exercise) and a trend towards a decrease in HSL- LD (P = 0.063) *versus* pre-exercise.

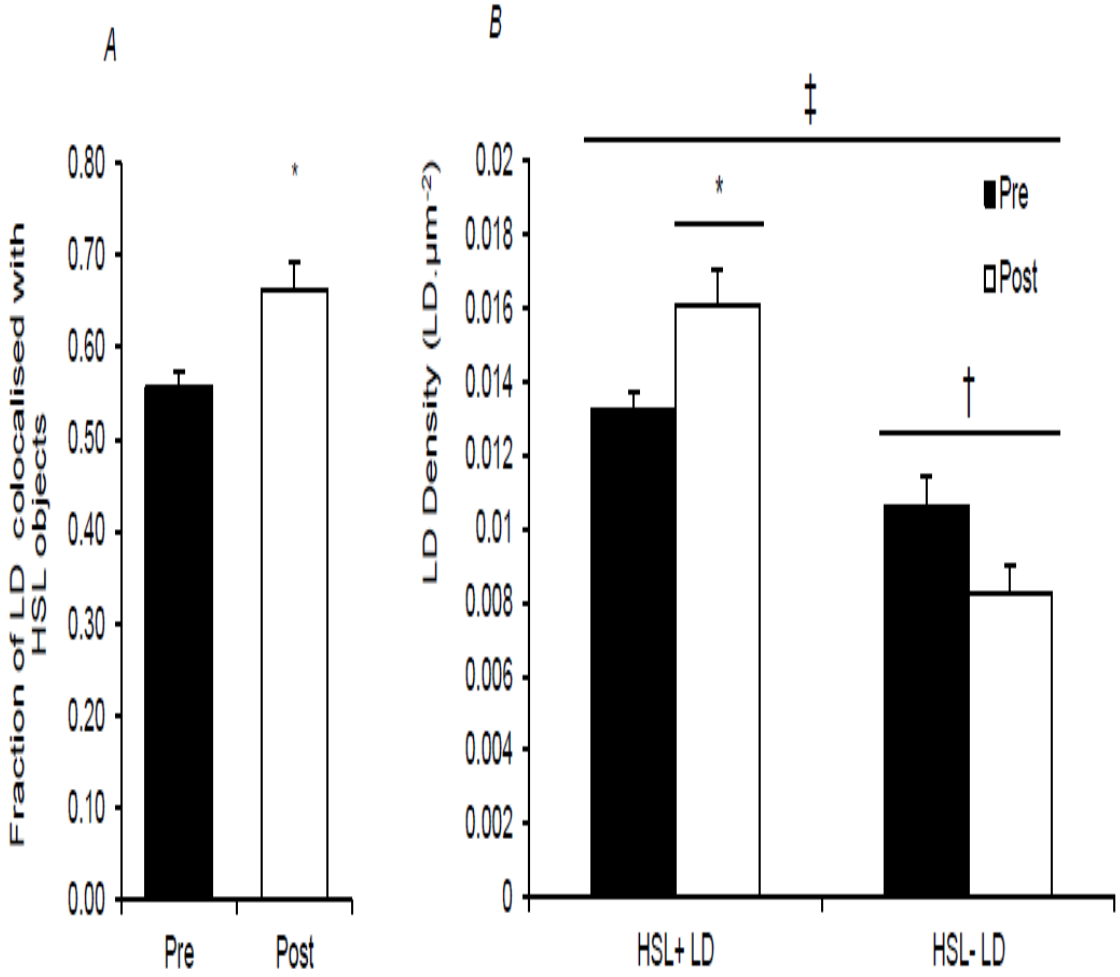

Figure 4. ATGL distribution does not change from pre to post-exercise as visualised through immunofluorescence microscopy.

Representative images of ATGL, PLIN2 and LD pre and post-exercise obtained using a 63x oil objective of a confocal microscope (A). White bars represent 50 µm. LD were visualised using BODIPY 493/503 and represent IMTG stores within the cell. Muscle fibres that had the highest lipid droplet content were selected and analysed. An 8x digital magnification was then applied to the centre of these muscle fibres and images were obtained to identify and quantify distribution and colocalisation between ATGL and LD associated with either PLIN2 (B) or PLIN5. White bars represent 2 µm. Images A and B show that pre-exercise ATGL had punctate staining throughout the cell and this was unaltered post-exercise.

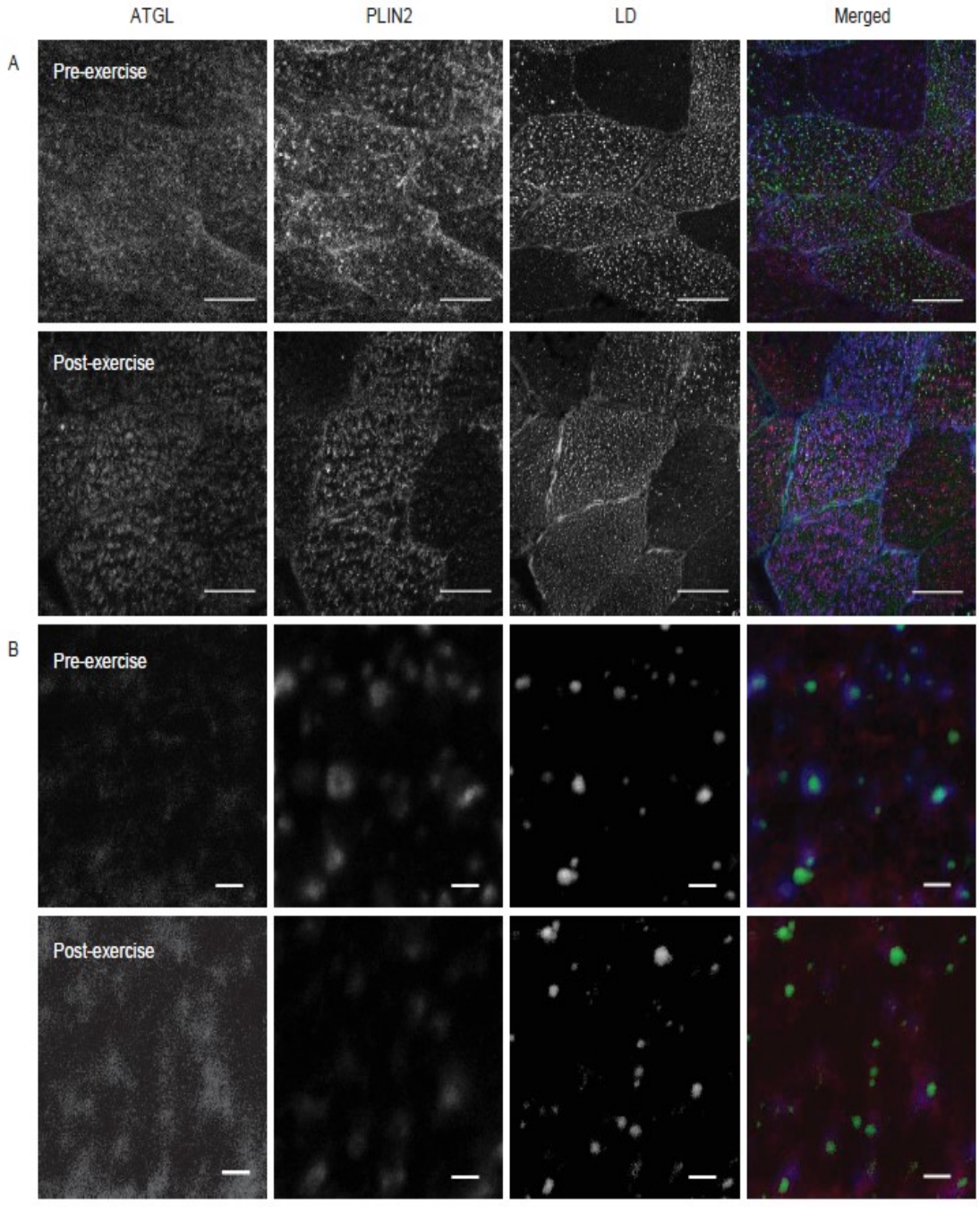

Figure 5. Immunofluorescence microscopy images of HSL, PLIN2/PLIN5 and LD pre and post-exercise.

Colocalisation between HSL, PLIN2 (A) or PLIN5 (B) and LD as visualised through immunofluorescence microscopy and quantified pre and post exercise. Images captured on a 63x oil objective of a confocal microscope at 16x digital magnification in the central region of fibres that had the highest lipid droplet content. White bars represent 2 μm. PLIN2 (A) and PLIN5 (B) were associated with LD or

located in the cytosol. HSL redistributes from larger storage clusters to a greater number of smaller, discrete clusters centred on different subclasses of LD (i.e. PLIN+ or PLIN- LDs).

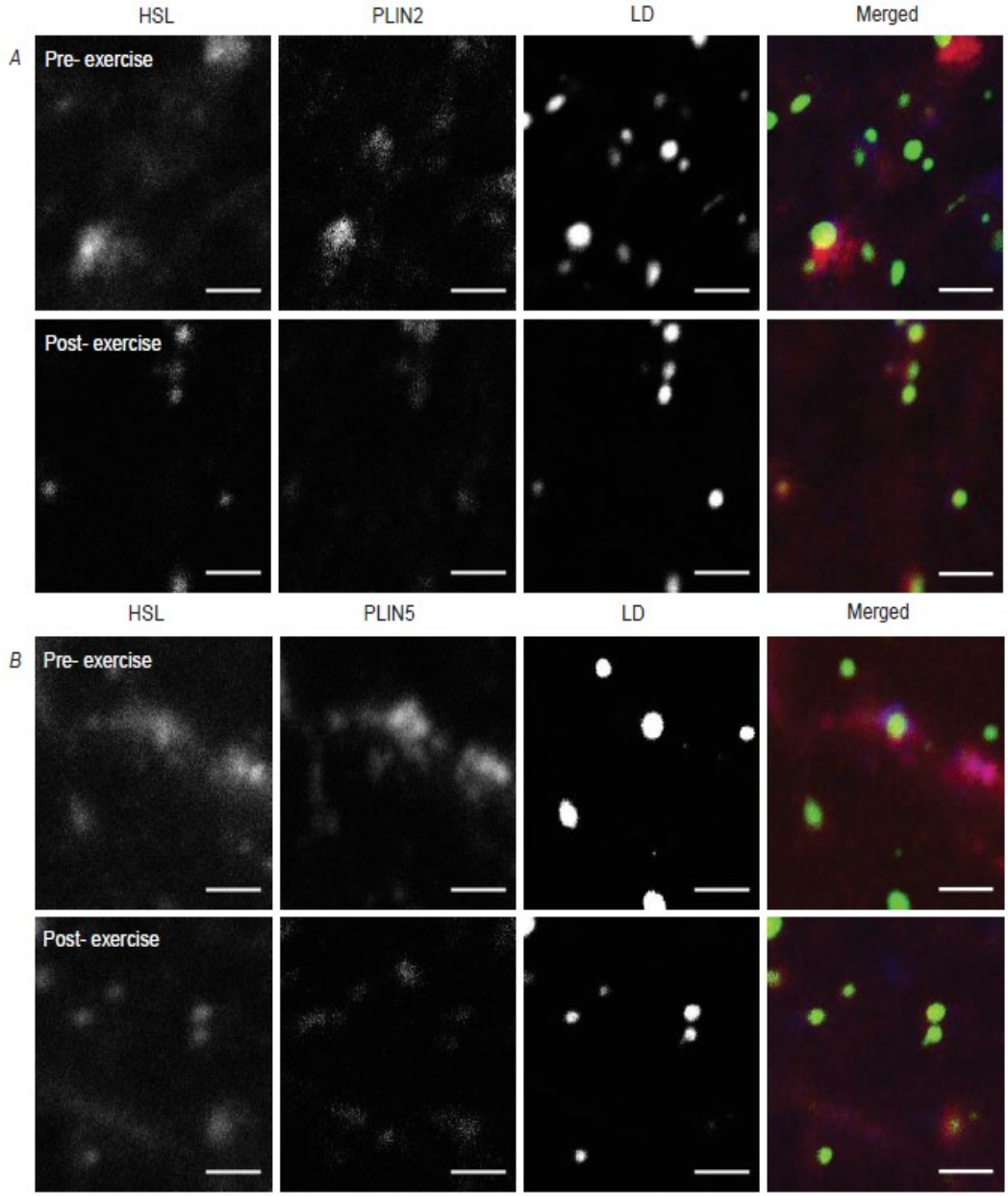

Figure 6. HSL preferentially redistributes to PLIN5+ LD from pre to post-exercise.

HSL colocalisation with different LD pools (PLIN+ or PLIN- LDs) was quantified from immunofluorescence microscopy images of HSL, LD and PLIN2 (A) or PLIN5 (B) pre and post- exercise. Data were collected as averages of 15 fibres per participant per time point. Values are presented as means ± SEM (n = 8 per group). * Main effect for exercise (P < 0.05 *vs.* pre-exercise). †Main effect for PLIN association to LD (P < 0.05 *vs.* PLIN- LD). ‡ Main interaction effect for PLIN5 association to LD (P < 0.05 *vs.* PLIN5- LD).

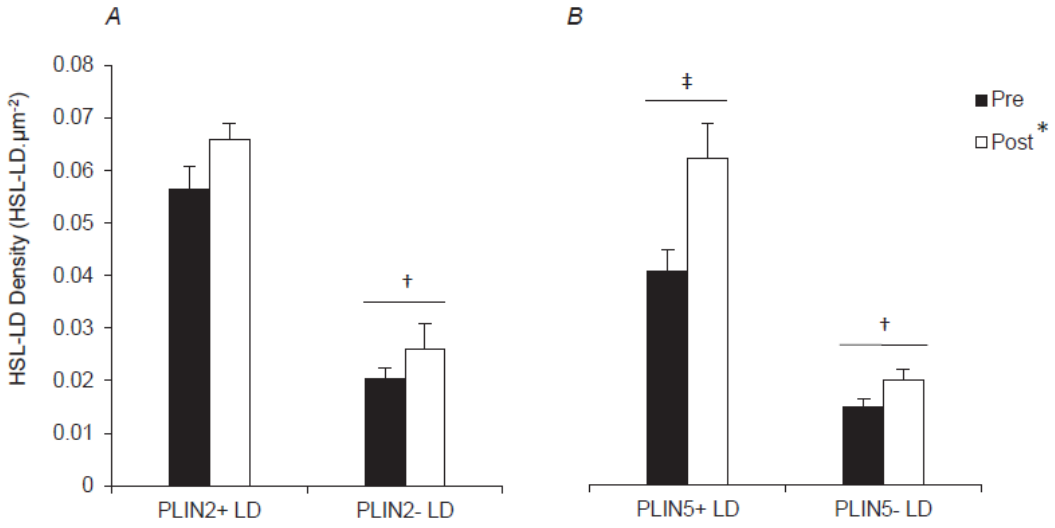

Figure 7. ATGL colocalisation with different pools of LD does not change from pre to post-exercise

ATGL colocalisation with different LD pools (PLIN+ or PLIN- LDs) was quantified from immunofluorescence microscopy images of ATGL, LD and PLIN2 (A) or PLIN5 (B) pre and post- exercise. Data were collected as averages of 15 fibres per participant per time point. Values are presented as means ± SEM (n = 7 per group). †Main effect for PLIN association to LD ($P < 0.05$ *vs.* PLIN-LD).

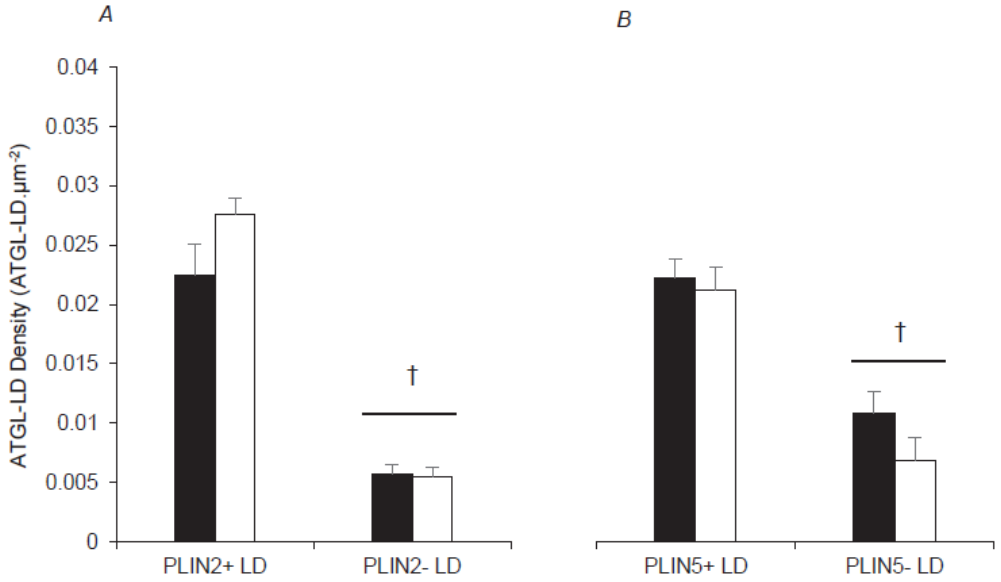

TABLE 2. Substrate utilisation during 60 min cycling at ~60% $\dot{V}o_{2peak}$

	15 min	30 min	45 min	60 min	Overall
Heart rate (beats.min^{-1})	134 ± 3	139 ± 5	139 ± 4	139 ± 6	138 ± 4
Percentage of $\dot{V}o_{2peak}$	58 ± 2	59 ± 2	60 ± 2	58 ± 2	59 ± 2
RER	0.88 ± 0.01	0.86 ± 0.01	0.86 ± 0.01	0.85 ± 0.01	0.86 ± 0.01
CHO oxidation (g.min^{-1})	1.48 ± 0.08	1.38 ± 0.08	1.36 ± 0.1	1.26 ± 0.09	1.37 ± 0.07
(percentage of total oxidation)	61.7 ± 3.4	57.2 ± 3.6	23.34 ± 1.8	52.8 ± 4.2	56.6 ± 3.1
Fat oxidation (g.min^{-1})	0.43 ± 0.05	0.49 ± 0.06	0.52 ± 0.05	0.54 ± 0.07	0.49 ± 0.05
(percentage of total oxidation)	40.1 ± 3.3	44.5 ± 3.5	47 ± 3.12	48.9 ± 4.1	45.1 ± 3.1